THE EFFECT OF ELEVATED TEMPERATURE HISTORY ON PROPERTIES AND HYDRATION OF HARDENED CEMENT PASTE

Go IGARASHI
Graduate School of Environmental Studies, University of Nagoya, Japan

Nobuyuki TAKAMATSU
Graduate School of Environmental Studies, University of Nagoya, Japan

Kazuo YAMADA
Research & Development Center: Taiheiyo Cement Corporation, Japan

Ippei MARUYAMA
Associate Prof., Graduate School of Environmental Studies, University of Nagoya, Japan

ABSTRACT:
The effect of elevated temperature history due to heat of hydration on physical properties and hydration system in the cement paste were investigated. The elevated temperature in early ages is known to cause stagnation of strength development. Therefore, the degree of hydration of each mineral component as well as hydrates is determined by X-ray Rietvelt analysis, and cement paste properties, namely, chemically bound water, density of hardened cement paste, specific surface area and strength were investigated. As a results, up to 28 days, strength of cement paste with/without elevated temperature can be evaluated with gel/space ratio of cement paste system.
Keywords: hardened cement paste, early age, elevated temperature history, hydration process, phase composition, strength

1. INTRODUCTION

The properties of concrete depend on the intrinsic properties of cement, condition of curing environment, and the condition or properties of aggregate. From these back ground, several simulation models of hydration process and various properties of concrete based on the hydration models are proposed so far [1][2][3][4].
The simulation model, "CCBM" has been developed by the one of the authors, which is improved from the simulation model of unreacted core model proposed by Tomosawa [5][6][7].
However, there is little information about the effect of the hydration of cement and phase composition on properties subjected to elevated temperature history in early age. Therefore, for the precise modeling, the hydration data with elevated temperature history is long-awaited.
In this study, the effect of elevated temperature history on phase composition, development of capillary water, specific surface area and compressive strength of hardened cement paste were investigated for intending the improvement of hydration model.

2. EXPERIMENTS

2.1 Cement and Mixture proportion

The ordinary Portland cement were used for this study. The properties of the cement are shown in Table 1. Cement pastes were mixed with omni mixer, and its water to cement ratio is 0.40 or 0.55 (notation: 40, 55). Remixing was conducted for taking bleeding. Specimens were sealed with adhesive aluminum tape and were placed in the room of 20±1 ^{o}C or in temperature controlled chamber which is simulating elevated temperature history in full-scale column.

2.2 Condition of curing temperature

Specimens in the temperature controlled chamber were subjected to the maximum of 60 ^{o}C in temperature history. This temperature history is determined according to the measurement of temperature history in the center of a 1m^3 concrete specimen. The property of hydration heat varies according to amount of cement, temperature of fresh concrete, amount of Superplasticizer and so on. However, in this study, the same elevated temperature history was applied regardless of water to cement ratio for the sake of comparison the temperature dependency of cement paste. The elevated temperature history is shown in Fig.1.

Table 1 Property of cement

Cement	Density (g/cm^3)	Blaine (cm^2/g)	Ig.loss (%)	Chemical composition (%mass)								
				SiO_2	Al_2O_3	Fe_2O_3	CaO	MgO	SO_3	Na_2O	K_2O	Cl^-
OPC	3.16	3110	0.64	21.8	4.49	2.90	63.9	1.84	2.26	0.20	0.38	0.007

The series of curing under constant temperature of 20 °C is called 20 °C condition and notation of 'N4020' and 'N5520' is used for Normal Portland cement paste with w/c=0.4 and 20 °C condition and that with w/c=0.55 and 20 °C condition. Likewise, the series of curing with elevated temperature history is called 60 °C condition and notaion of 'N4060' and 'N5560' is used in this paper.

2.3 Sample preparing

The samples whose hydration process was ceased at each target concrete age were used for determining hydration ratio and amount of chemically bound water.
Analysis samples were prepared as follows: Mix the materials at the specified temperature and seal-cure until the specified age. Crash the specimen to an appropriate size with a hammer and finely pulverize with acetone using a disk mill. After separating the powder from acetone by suction filtration, dry the sample for approximately two weeks in an environment of 15%RH, to obtain a hydration analysis sample.

2.4 Measured Properties

(1) Compressive strength

Compressive strength were tested at 1, 3, 7, 14 and 28 days.
Specimen is cylindrical shape with the dimension of φ 50×100mm. The data is averaged values of three specimens at each age.

(2) Evaporable water, density of hardened cement paste, and total pore volume

The amount of water content, total pore volume which can be filled with water, and density of hardened cement paste (hcp) at each age were measured.
At each age, hcp was crushed into about 8mm^3 (about 1g), and the mass of these samples were measured. Afterwards, the samples were saturated sufficiently by using vacuum pump. The mass and nominal density of hcp which is under saturated surface-dry condition by Archimedes method. Thereafter, this sample was dried off at 105 °C for 24 hours and mass of samples were weighed in absolutely dry condition. The mass of these samples were measured with electronic balance whose accuracy is 0.1mg, and calculated density of hcp with total pore volume and nominal density of saturated hcp.

(3) Chemical shrinkage

The chemical shrinkage was measured according to the method proposed by JCI Committee [8]. Three specimens were prepared for each condition.
Cement paste whose water to cement ratio of 0.40 was packaged as a thickness of about 20 mm, and paste whose water to cement ratio of 0.55 was packaged as a thickness of about 40 mm into jar. Saturated solution with calcium hydroxide was used for additional water. Essentially, chemical shrinkage develops immediately after pouring water, however, in this study, chemical shrinkage was zeroed at one hour after mixing.
Curing temperature was settled at constantly 20 °C.
The series of 60 °C is not investigated, because there is no way to measure under condition of temperature change.

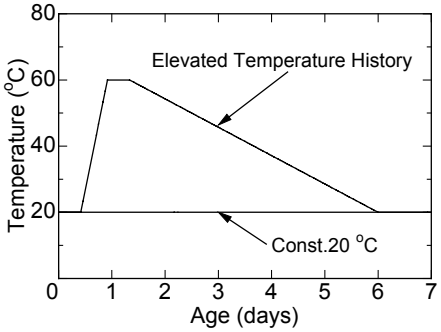

Fig.1 Elevated temperature history

(4) Specific surface area of hcp

The sample which was dried off at 105 °C in section (2) was used for measuring isothermal adsorption and specific surface area of hcp [9] as well.
Isothermal adsorption curve was measured by volumetric method [10] (Hydrosorb1000, Quantachrome Co.).
The mass of adsorption was measured from 5%RH to 95%RH at intervals of 5%RH.

(5) XRD/Rietveld method

The X-ray diffraction (XRD) had been conduced and that result are used for Rietvelt analysis. The procedures proposed by Hoshino *et al* are followed [11].
The measurement conditions of XRD were a tube voltage of 50kV, tube current of 250 mA, scan range of 2θ = 5 to 65°, step width of 0.02°, and scan speed of 2°/min. The software used for Rietveld analysis was TOPAS (Bruker AXS). The phases that were quantified were calcite, gypsum, bassanite, portlandite, ettringite (AFt), monosulfate (AFm), as well as basic minerals such alite (C_3S), belite (C_2S), cubic-C_3A, orthorhombic-C_3A, and C_4AF.
Structural models for clinker minerals (alite, belite, cu-C_3A, or C_3A, and C_4AF) were taken from the NIST Technical Report (Stutzman *et al.* 2002). Those for the calcite, gypsum, bassanite, CH, AFt, AFm and corundum were taken from the ICSD database (Fachinformationszentrum 2006). A halo pattern of amorphous phase was refined as a background function. The amount of amorphous phase is calculated by Eq. (1).

$$A = \{100 \times (S_R - S)\} / \{S_R \times (100 - S)/100\} \quad (1)$$

where,

A : the amount of amorphous phase (mass%)
S : the added ratio of corundum (mass%)
S_R : the measured value of corundum (mass%)

To evaluate reaction ratio of each mineral and phase composition in hcp, the composition under each drying condition were supposed as Table 2, and convert into anhydride and calculate hydration ratios at 0.5, 0.75, 1, 3, 7, 14 and 28 days.

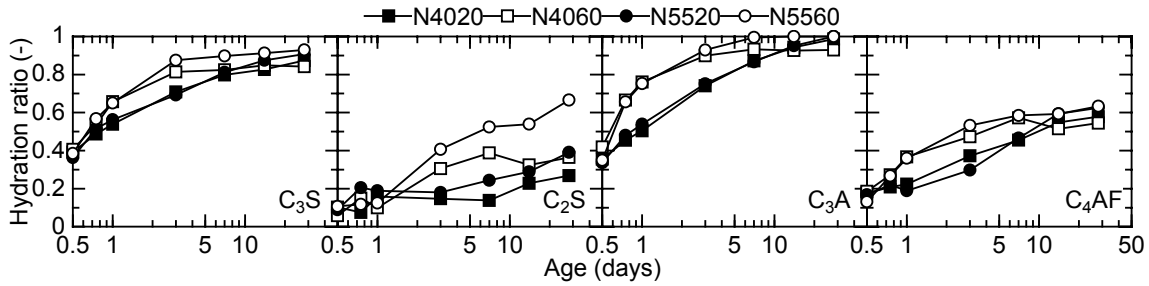

Fig.2 Hydration ratio of each mineral in cement paste

(6) Chemically bound water

The chemically bound water was calculated from the mass difference from 105 °C to 1000 °C obtained by the thermal gravity and differential thermal analysis (TG-DTA).

3. RESULTS AND DISCUSSIONS

3.1 Hydration process of cement paste

Fig.2 shows the hydration ratio of each mineral from the result of XRD/Rietveld method. The hydration ratio of 60 °C condition developed rapidly compared to the those of 20 °C condition. The effect of water to cement ratio was not found obviously for C_3S, C_3A and C_4AF. However, the grate discrepancy was observed with regard to the case of C_2S in 60 °C condition. Hydration of N5560 was faster than N4060. Taking into consideration that self-desiccation of N40 occurs earlier than N55 due to the lower w/c ratio, this lower chemical potential of water may affect hydration process of C_2S.

The phase composition was calculated based on these hydration data. In the calculation procedure, CaO/SiO_2 molar ratio (Ca/Si ratio) is treated as variable in the process, because it is generally known that Ca/Si ratio vary in hydration process [12].

In this study, the phase composition was identified by convergence as follows. The flowchart is shown in Fig.3.

First, each phase in cement paste are converted into anhydride. Then, the amount of C-S-H value and Ca/Si ratio of C-S-H are supposed temporary value.

Second, the amount of remainder between solute and hydrated as crystals of Al_2O_3 and Fe_2O_3 are calculated. Then, the remainder of Al_2O_3 and Fe_2O_3 values are supposed to affect formations of C-A-H or C-F-H in amorphous.

Third, the amount of remainder between solute and hydrated as crystals of CaO and SiO_2 are calculated based on Rietveld analysis. Then, the remainder of CaO and SiO_2 are supposed to be used in the formations of C-S-H.

Forth, Ca/Si ratio of C-S-H is calculated and converted all amorphous into anhydride.

Finally, phase composition can be identified as the value at convergence by repetition above calculation.

The evolution of phase composition as volumetric ratio, which is under sealed condition, is shown in Fig.4. The validity of this calculation was verified from the aspect of chemically bound water, density of hcp and chemical shrinkage as shown in Fig.5, Fig.6, and Fig.7 respectively.

Table 2 Composition of hydration product under each drying condition

Product	Drying Condition	H/C ratio	Composition	Molecular Weight (g)	Density (g/cm^3)
C-S-H	1000 °C	0	C_xSH_0	155	-
	105 °C	0.88	$C_xSH_{1.5}$	182	2.65
	15%RH,20 °C	1.18	C_xSH_2	191	2.40
	Saturated	1.18	C_xSH_2	191	2.40
AFt	1000 °C	0	$C_6A\hat{S}_3H_0$	679	-
	105 °C	2.00	$C_6A\hat{S}_3H_{12}$	895	2.38
	15%RH,20 °C	5.30	$C_6A\hat{S}_3H_{31.8}$	1252	1.73
	Saturated	5.33	$C_6A\hat{S}_3H_{32}$	1255	1.77
AFm	1000 °C	0	$C_4A\hat{S}H_0$	406	-
	105 °C	2.00	$C_4A\hat{S}H_8$	550	2.40
	15%RH,20 °C	2.90	$C_4A\hat{S}H_{11.6}$	615	2.01
	Saturated	3.00	$C_4A\hat{S}H_{12}$	623	1.90
C-A-H	1000 °C	0	C_4AH_0	326	-
	105 °C	2.00	C_4AH_8	470	2.70
	15%RH,20 °C	3.25	C_4AH_{13}	561	-
	Saturated	3.25	C_4AH_{13}	561	2.02
C-F-H	1000 °C	0	C_4FH_0	384	-
	105 °C	2.00	C_4FH_8	528	2.70
	15%RH,20 °C	3.25	C_4FH_{13}	618	-
	Saturated	3.25	C_4FH_{13}	618	2.23

where, C : CaO, S : SiO_2, A : Al_2O_3, F : Fe_2O_3, H : H_2O, $\hat{S}$: SO_3.
* The shown value of C-S-H is the value when x is 1.7.

The comparison between measured value and estimated value from phase composition based on Rietveld analysis is shown in Fig.5, Fig.6 and Fig.7.

In Fig.5, estimated value shows little lower than measured value, but overall trend are correspondent comparatively. In the case of density of hcp in Fig.6, small discrepancy is seen in very early age, but predicted values from X-ray/Rietvelt analysis shows good agreement with measured values. Regarding chemical shrinkage in Fig.7, predicted values are higher than the measured values in very early age, but they also shows relatively good agreement with measured value. It should be noted that material balance, especially Calcium, can be wrong because chemical shrinkage measured in saturated solution with calcium hydroxide, but XRD sample was cured in sealing.

3.2 Specific surface area

The experimental results of vapor isothermal adsorption is shown in Fig.8. The value of surface area calculated with the BET theory is shown in Fig.9. In Fig.9 it is shown that surface area under 60 °C condition increases dramatically in early age, whereas, surface area under 60 °C condition is still lower than that under 20 °C condition at 28 days regardless of that hydration ratio of each minerals in cement paste under 60 °C condition is the same or larger than those under 20 °C condition as shown in Fig.2. This phenomenon indicates that C-S-H

structure which is formed during the high temperature period, is different from that formed under 20 °C.
For the discussion of this trend from the point of view of Ca/Si ratio in C-S-H, the time dependent behavior of evaluated Ca/Si ratio is shown in Fig.10.
Fig.10 shows that Ca/Si ratio of C-S-H under 60 °C condition decrease rapidly during the high temperature period and the value is temporarily lower than 20 °C condition. After that, Ca/Si ratio increase after 7days when the curing temperature is backed to 20 °C, and at this point, the value of Ca/Si ratio of 60°C condition is higher than that of 20 °C condition.
The relationship between Ca/Si ratio and calculated specific surface area of C-S-H is shown in Fig.11. For this calculation, it was supposed that surface area of hcp was equal to surface area of C-S-H.
Fig.11 shows that as Ca/Si ratio become lower, surface area of C-S-H become higher. This trend was already observed in surface area obtained by nitrogen adsorption by Saeki *et al*. [14].
In this study, the value of Ca/Si ratio was obtained from iterative calculation method as shown in section 3.1, accordingly, it changes widely by supposition of hydration product of Al_2O_3 and Fe_2O_3. Actually, the true value of Ca/Si ratio should be evaluated with transmission electron microscope. However, this trend can be obtained when the different C-A-H or C-F-H composition is assumed.
The calculation values of specific surface area of 0.5 day (Circle area in Fig.11) were larger than approximated curve in Fig.11. This phenomenon agrees with the published literature, which is surface area of hydration product decrease until 14hours [15].

3.3 Compressive Strength

The development of the compressive strength of hcp is shown in Fig.12. This figure shows compressive strength under 60 °C condition is higher than 20 °C

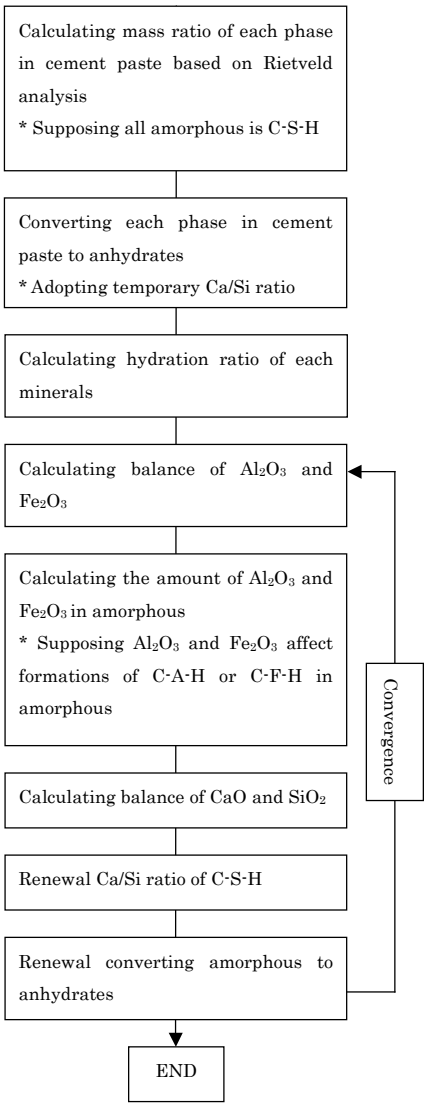

Fig.3 Flowchart of convergence

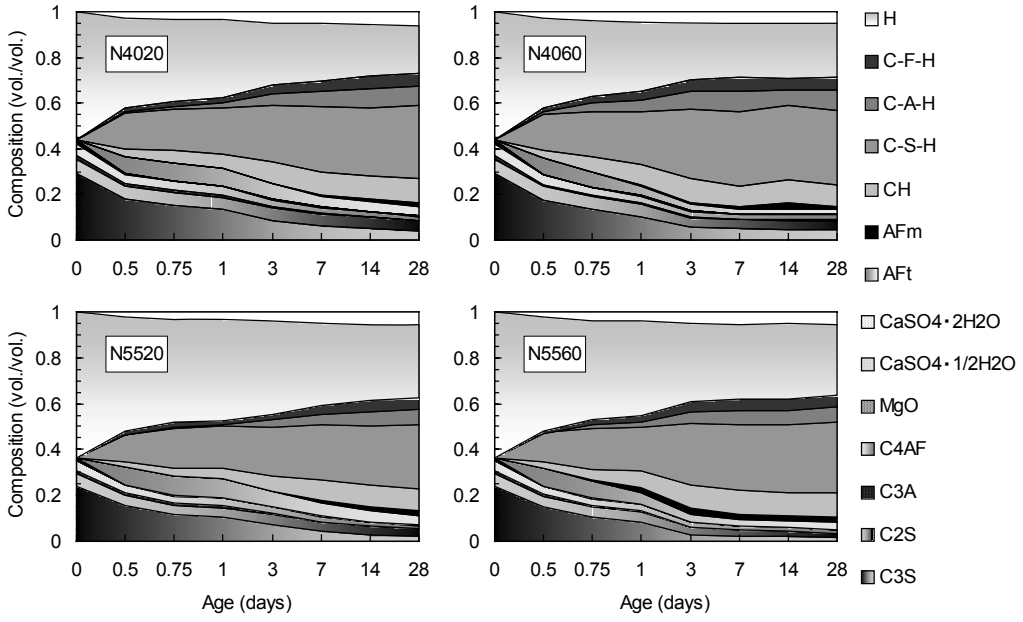

Fig.4 Phase composition of hardened cement paste

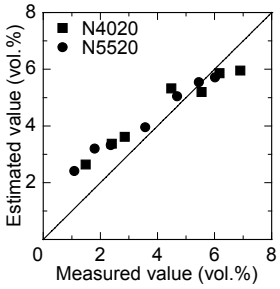

Fig.5 Chemical shrinkage

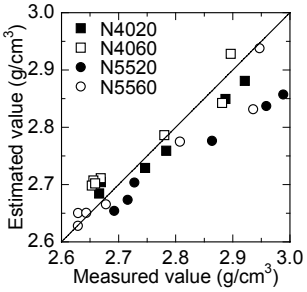

Fig.6 Density of hcp

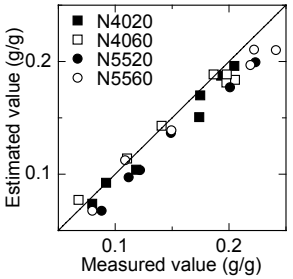

Fig.7 Chemically bound water

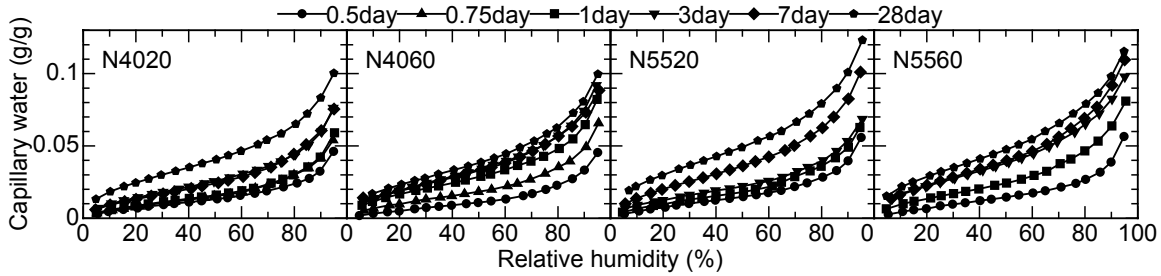

Fig.8 Isothermal adsorption of hardened cement paste

condition during 28 days. As with previous study by Sakai *et al*. [16], relationship between compressive strength and gel/space ratio based on the phase composition is discussed, for the evaluation of the effect of elevated temperature history on the compressive strength of hcp [17].

$$X(t) = \frac{V_{hydrates}(t)}{V_{hydrates}(t) + V_{pore}(t)} \quad (2)$$

$$S(t) = S_0 X(t)^N \quad (3)$$

where,

$X(t)$: gel/space ratio (vol./vol.)
$V_{hydrates}(t)$: the volume of hydration product (vol.%)
$V_{pore}(t)$: the volume of pore volume of hardened cement paste (vol.%)
$S(t)$: strength (MPa)
t : age
S_0 : constant (MPa)
N : constant (-)

The relationship between compressive strength and gel/space ratio is shown in Fig.13. It is good relationship was observed when S_0 and N were supposed as 279MPa and 4.0 respectively. These supposed values are higher than the values of analysis by Sakai. This can be explained by the model of phase composition. And it is confirmed that the relationships between gel/space ratio and compressive strength are on the similar curve regardless of curing temperature history.

4. CONCLUSIONS

In this study, degree of hydration, phase composition, and physical properties of hardened cement paste with water to cement ratio of 0.40 and 0.55, and different

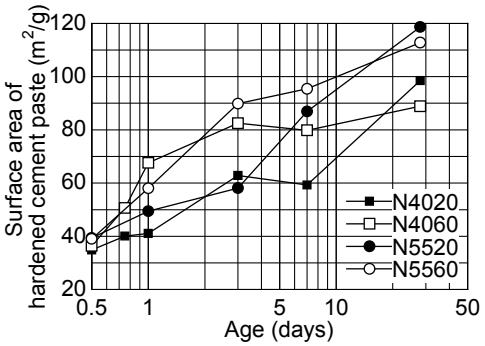

Fig.9 Development of surface area

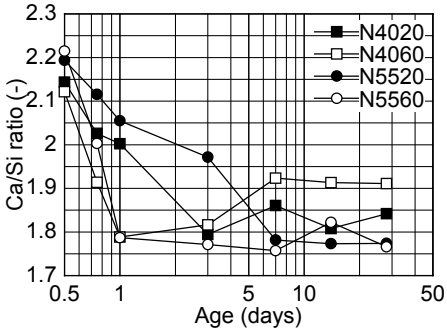

Fig.10 Development of calculated Ca/Si ratio

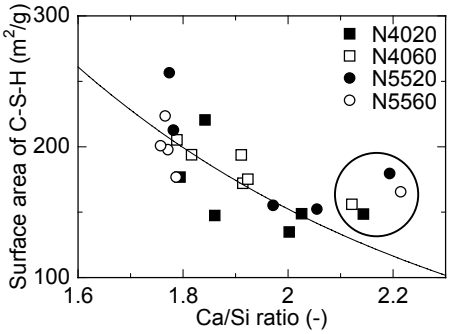

Fig.11 Relationship between Ca/Si ratio and surface area

curing temperature history were investigated. The following conclusions are drawn from the limit of the present study:

(1) The phase composition calculation method based on Rietveld Analysis is proposed, and the result of this method can comparatively evaluate chemical shrinkage, chemically bound water and density of hardened cement paste without very early age.
(2) Accordingly, the proposed model can calculate the evolution of CaO/SiO_2 molar ratio of C-S-H produced in hardened cement paste.
(3) Relationship between calculated CaO/SiO_2 molar ratio of C-S-H and calculated specific surface area of C-S-H shows that decrease of CaO/SiO_2 molar ratio increases the specific surface area of C-S-H.
(4) Compressive strength of hardened cement paste can be evaluated by gel/space ratio regardless curing temperature history. This results is based on the assumptions of the proposed phase composition model.

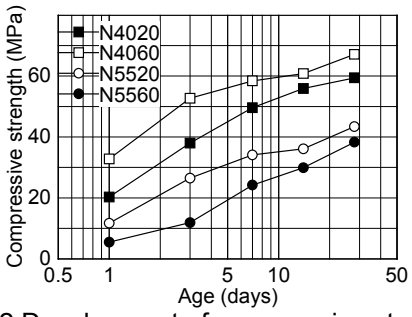

Fig.12 Development of compressive strength

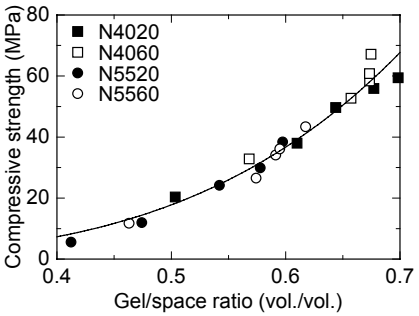

Fig.13 Relationship between compressive strength and gel/space ratio

ACKNOWLEDGEMENT

The authors would like to express their sincere thanks to Dr. Yoshifumi Hosokawa, Mr. Takahito Nozaki, and Ms. Haruka Takahashi (Research & Development Center, Taiheiyo Cement Corporation) for their supports.

REFERENCES

1. Maekawa, K., *et al*., "Multi-scale Modeling of Concrete Performance: Integrated Material and Structural Mechanics," J. Adv. Conc. Tech., Vol.1, No.2, pp.91-126, 2003.
2. K. van Breugel, "Simulation of hydration and formation of structure in hardening cement-based materials," Ph.D thesis 2nd ed., TU Delft, p.35, 1997.
3. D. P. Bentz, *et al*., "Prediction of Adiabatic Temperature Rise in Conventional and High-Performance Concrete Using a 3-D Microstructural Model," Cem. Conc. Res. 28, No.2, pp.285-297, 1998.
4. Navi, P. & Pignat, P., "Simulation of cement hydration and the connectivity of the capillary pore space," Advanced Cement Based Materials, 4, 2, pp. 58-67, Nov. 1996.
5. Tomosawa, F., "A Hydration Model of Cement, Proceedings of Annual Meeting on Cement Technology," Cement Association of Japan, 28, pp.53-57, 1974.
6. Maruyama, I., *et al*., "Prediction of Adiabatic Temperature Rise in Portland Cement Concrete Using Computational Cement Based Material Model," J. Structural and Construction Eng. Transactions of AIJ, Vol.600, pp.1-8, Feb. 2006.
7. Maruyama, I., *et al*., "Prediction of Temperature and Moisture Distribution in High-Strength Mass Concrete Based on Heat and Moisture Transport Model," J. Structural and Construction Eng. Transactions of AIJ, Vol.609, pp.1-8, Nov. 2006.
8. Japan Concrete Institute, The Report by the JCI Autogenous Shrinkage Committee, pp.44-50, Sep. 2002.
9. S. Brunauer, P. H. Emmett, E. Teller, "Adsorption of Gases in Multimolecular Layers," J. American Ceramic Society, Vol.60, pp.309-319, 1938.
10. Ono, Y., Suzuki, I. The Chemistry of Adsorption and Application, Kodansya Scientific, pp.42-46, 2003.
11. Hoshino, S., Yamada, K., Hirao, H., "XRD/Rietveld Analysis of the Hydration and Strength Development of Slag and limestone Blended Cement," Journal of Advanced Concrete Technology, Vol.4, No.3, pp.357-367, 2006.
12. Nishikawa, T., Suzuki, K., "Chemical Conversion of C-S-H in Concrete," Cem. Conc. Res. Vol.24, pp.176-182, 1994.
13. A. Bentur, *et al*., "Structural Properties of Calcium Silicate Paste: II, Effect of Curing Temperature," J. Amer. Ceram. Soc., Vol.62, No.7-8, pp.362-366, 1979.
14. Sasaki, K., Saeki, T., "Effect of Chemical Composition of C-S-H on Concrete Durability," Journal of the Society of Materials Science, Japan Vol.56, No.8, pp.699-706, Aug. 2007.
15. H. M. Jennings, "A model for the microstructure of calcium silicate hydrate in cement paste," Cem. Conc. Res., Vol.30, pp.101-116, 2000.
16. Sakai, E., Imoto, H., Daimon, M., "Phase Composition and Strength Development of Blast Furnace Slag Cement," Proceedings of the Japan Concrete Institute Vol.26, No.1, pp.135-140, 2004.
17. T. C. Powers, "Structure and Physical Properties of ;Hardened Portland Cement," J. Amer. Ceram. Soc., Vol.40, pp.1-6, 1958.